



Free vibration analysis of cracked beams by a combination of finite elements and component mode synthesis methods

M Kisa^a, J Brandon^{a,*}, M Topcu^b

^a*Division of Mechanical Engineering and Energy Studies, Cardiff School of Engineering, University of Wales, Cardiff, U.K.*

^b*Department of Mechanical Engineering, Pamukkale University, Turkey*

Received 25 May 1997; accepted 1 January 1998

Abstract

Previous work on the dynamics of defective structures, by the authors' colleagues and other studies in the literature, has revealed substantial variability in predicted vibration behaviour depending on the interface conditions. In the current project the authors have set out to develop a strategy which retains the maximum amount of common information concerning the linear regions of the structure, whilst allowing the maximum scope to vary conditions at the (nonlinear) interface.

In this paper, the vibrational characteristics of a cracked Timoshenko beam are analysed. The study integrates the finite element method and component mode synthesis. The beam divided into two components related by a flexibility matrix which incorporates the interaction forces. These forces can be derived from fracture mechanics theory as the inverse of the compliance matrix calculated using stress intensity factors and strain energy release rate expressions. Each substructure is modelled by Timoshenko beam finite elements with two nodes and 3 degrees-of-freedom (axial, transverse and rotation) at each node. © 1998 Elsevier Science Ltd. All rights reserved.

Keywords: Finite element, Component mode synthesis, Crack, Modal analysis, Timoshenko beam

Nomenclature

a	crack length	\mathbf{K}_{el}	stiffness matrix for Timoshenko beam element
A, B	components	\mathbf{K}_{cr}	stiffness matrix for crack element
u, v	displacements with respect to x - and y -axes	c_{ij}	compliance coefficients
ψ	deflection	$\mathbf{M}, \mathbf{C}, \mathbf{K}$	mass, damping and stiffness matrix
L	length of the element	q	generalised displacement
κ	shear correction factor	$f(t)$	external force
G	shear modulus	ω	natural frequency
E	Young's modulus of elasticity	ϕ	modal matrix
I_y	section moment of inertia with respect to y -axis	Ψ	mass normalised modal matrix
		p, s	principal coordinates
		\mathbf{m}_m	modal mass
		\mathbf{k}_m	modal stiffness
		T, U	kinetic and strain energy
		U_c	strain energy of connectors
		\mathbf{K}_c	connector matrix

* To whom all correspondence should be addressed.

1. Introduction

The effect of cracks on the dynamic behaviour of structural elements has been the subject of several investigations. Any accidental (such as cracks) or intentional modification in a structure will affect its dynamical behaviour and change its stiffness and damping properties. Consequently, the natural frequencies and mode shapes of the structure contain information about the location and dimensions of the damage. Gudmundson [1,2] investigated the influence of small cracks on the natural frequencies of slender structures by a perturbation method as well as by a transfer matrix approach. Cawley and Adams [3] have combined sensitivity analysis and the finite element method to determine crack location. Yuen [4] proposed a systematic finite element approach to determine the relationship between damage location, damage size and the corresponding changes in the eigen parameters of a cantilever beam. Gounaris and Dimarogonas [5] suggested a finite element model for dynamic analysis of an edge-cracked beam. In this work, in order to consider the discontinuity in both deflection and slope due to the crack, two different shape functions were needed for two segments separated by the crack. Qian et al. [6] developed a finite element model of an edge-cracked beam. They derived the stiffness matrix for a cracked beam element by energy method. This stiffness was given two values, one for the closed crack and the other for the open crack. The sign of the stress on crack faces determines the appropriate value, therefore, the equation of motion was nonlinear requiring a numerical method. Rizos et al. [7] modelled the crack as a massless rotational spring, whose stiffness was calculated by using fracture mechanics. Shen and Taylor [8] developed an identification procedure to determine the crack characteristics from vibration measurements. Shen and Chu [9] proposed a modified crack beam theory and simulated numerically the dynamic response of simply supported beams having a fatigue crack. Ruotolo et al. [10] conducted a harmonic analysis of a cantilever beam with a closing crack using a finite element model of the Euler beam. Very recently, Abraham and Brandon [11,12], Brandon and Abraham [13] presented a method of utilising substructure normal modes to predict the vibration properties of a cantilever beam with a closing crack.

The full eigensolution of a structure containing substructures each having large numbers of degrees-of-freedom can be cumbersome and costly in computing time. A method proposed by Hurty [14] enabled the problem to be broken up into separate elements and thus considerably reduced its complexity. His method consisted of considering the structure in terms of substructures and was called as 'substructuring'. Essentially, the method required the derivation of the

dynamic equations for each component and these equations were then connected mathematically by matrices which represent the physical displacements of interface connection points on each component. In this way, one large eigenproblem is replaced by several smaller ones.

In many respects, the original rationale for such substructuring techniques has been rendered obsolete by the widespread availability of high performance computers. However, there are applications where alternative justifications are valid, for example where the results of independent analysis of individual structural modules are to be used to predict the dynamics of an assembled structure. In the present context the authors wish to examine the response prediction of an assembled structure under a variety of assumptions concerning nonlinearity at the interface of substructures which are otherwise linear. As has been mentioned, Abraham and Brandon have followed a similar strategy but with the characteristics of the interface modelled using much less sophisticated analytical assumptions [11–13].

The method used in this paper has been presented for *non-cracked* structures by Ewins [15], Martin and Ghlaïm [16], Ghlaïm [17], Moon and Cho [18] and Nobari et al. [19]. For a cracked Timoshenko beam, Abraham and Brandon [11] established an analytical method which is extended by current work using finite element method.

2. Theoretical model

The model chosen is a cantilever beam, of uniform cross-section A , having a transverse edge crack of depth a at a variable position ξ (Fig. 1).

The cantilever is divided into two components at the crack section leading to a substructure approach. The main advantage of this approach is that global nonlinear system with a local stiffness discontinuity is separated into two linear subsystems. Each component is also divided into finite elements with two nodes and 3 degrees-of-freedom at each node as shown in Fig. 2.

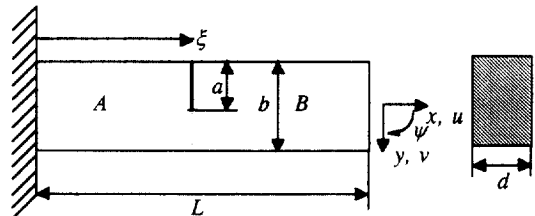


Fig. 1. Geometry of the cracked cantilever beam.

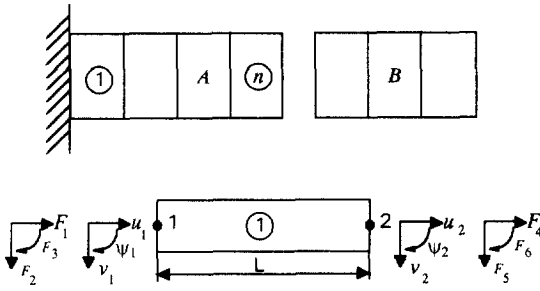


Fig. 2. Components of whole structure and dividing them into the finite number of elements.

2.1. Stiffness matrix of Timoshenko beam element

The analysis is developed from the procedure given by Gounaris and Papazoglou [20] adapted to 3 degrees-of-freedom for each node, $\delta = \{u, v, \psi\}$. In Fig. 2 representing a generic finite element, the applied system forces $F = \{F_1, F_2, F_3\}$ and the corresponding responses are shown. (Gounaris and Papazoglou give the stiffness matrix for the 2 degrees-of-freedom (v, ψ) for bending in the xy plane for a two-noded Timoshenko beam finite element [20]).

$$\mathbf{K}_I = \frac{EI_y}{L(L^2 + 12\alpha)} \times \begin{bmatrix} 12 & 6L & -12 & 6L \\ 6L & 4L^2 + 12\alpha & -6L & 2L^2 - 12\alpha \\ -12 & -6L & 12 & -6L \\ 6L & 2L^2 - 12\alpha & -6L & 4L^2 + 12\alpha \end{bmatrix} \quad (1)$$

where L is the length of an element, E is the Young's modulus of elasticity and I_y is the section moment of inertia with respect to the y -axis,

$$\alpha = \frac{EI_y}{\kappa GA} \quad (2)$$

κ is the shear correction factor, G is the shear modulus and A is the area of the cross-section of the element. The stiffness matrix for the 1 degree-of-freedom $\{u\}$ local axial displacement in the x -direction is [21],

$$\mathbf{K}_{II} = \frac{EA}{L} \begin{bmatrix} 1 & -1 \\ -1 & 1 \end{bmatrix}. \quad (3)$$

The total stiffness matrix for all the 3 degrees-of-freedom for each node and in accordance with the above \mathbf{K}_I , \mathbf{K}_{II} matrices according to displacement vector δ is now,

$$\mathbf{K}_{el} = \begin{bmatrix} \mathbf{K}_{II11} & & & \mathbf{K}_{II12} & & \\ & \mathbf{K}_{I11} & \mathbf{K}_{I12} & & \mathbf{K}_{I13} & \mathbf{K}_{I14} \\ & \mathbf{K}_{I21} & \mathbf{K}_{I22} & & \mathbf{K}_{I23} & \mathbf{K}_{I24} \\ \mathbf{K}_{II21} & & & \mathbf{K}_{II22} & & \\ & \mathbf{K}_{I31} & \mathbf{K}_{I32} & & \mathbf{K}_{I33} & \mathbf{K}_{I34} \\ & \mathbf{K}_{I41} & \mathbf{K}_{I42} & & \mathbf{K}_{I43} & \mathbf{K}_{I44} \end{bmatrix}_{(6 \times 6)} \quad (4)$$

2.2. The stiffness matrix for the crack

Considering the cracked node as a cracked element of zero length and zero mass [5], the crack stiffness matrix can be represented by equivalent compliance coefficients. The compliance matrix was taken from ref. [22], but adapted to the chosen beam element. The compliance coefficients matrix can be written according to the displacement vector $\delta = \{u, v, \psi\}$ as

$$\mathbf{C} = \begin{bmatrix} c_{11} & 0 & c_{13} \\ 0 & c_{22} & 0 \\ c_{31} & 0 & c_{33} \end{bmatrix}_{(3 \times 3)}. \quad (5)$$

The inverse of the compliance matrix \mathbf{C}^{-1} is the stiffness matrix of the nodal point. Therefore finally the stiffness matrix of the cracked nodal element can be written as

$$\mathbf{K}_{cr} = \begin{bmatrix} [\mathbf{C}]^{-1} & -[\mathbf{C}]^{-1} \\ -[\mathbf{C}]^{-1} & [\mathbf{C}]^{-1} \end{bmatrix}_{(6 \times 6)}. \quad (6)$$

3. Component mode analysis

Consider a component A . The equation of motion for this component is

$$\mathbf{M}_A \ddot{q}_A + \mathbf{C}_A \dot{q}_A + \mathbf{K}_A q_A = f_A(t) \quad (7)$$

where \mathbf{M}_A , \mathbf{C}_A and \mathbf{K}_A are mass, damping and stiffness matrices, respectively, for the component A , q and $f_A(t)$ are the generalised displacement and external force vectors, respectively. For undamped free vibration analysis, Eq. (7) becomes

$$\mathbf{M}_A \ddot{q}_A + \mathbf{K}_A q_A = f_A(t). \quad (8)$$

Assuming that

$$\{q\} = \{\phi\} \sin(\omega t + \beta), \quad \{\ddot{q}\} = -\omega^2 \{\phi\} \sin(\omega t + \beta) \quad (9)$$

and substituting them into Eq. (8), one ends up with the standard free vibration equation for the component A as,

$$\omega_A^2 \mathbf{M}_A \phi = \mathbf{K}_A \phi \quad (10)$$

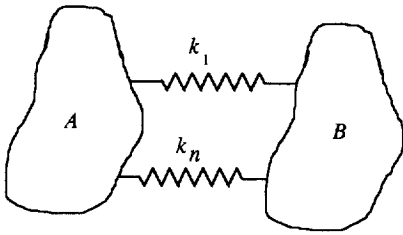


Fig. 3. Two components connected by springs.

which gives eigenvalues $\omega_A^2 1, \dots, \omega_{An}^2$ and modal matrix ϕ_A for the component A . Making the transformation

$$q_A = \phi_A p_A \tag{11}$$

where p_A is the principal coordinate vector. By premultiplying ϕ_A^T and substituting Eq. (11), Eq. (8) becomes

$$(\phi_A^T \mathbf{M}_A \phi_A) \ddot{p}_A + (\phi_A^T \mathbf{K}_A \phi_A) p_A = \phi_A^T f_A(t) \tag{12}$$

where

$$\begin{aligned} \phi_A^T \mathbf{M}_A \phi_A &= [\mathbf{m}_m] \\ \phi_A^T \mathbf{K}_A \phi_A &= [\mathbf{k}_m] \end{aligned} \tag{13}$$

where $[\mathbf{m}_m]$ and $[\mathbf{k}_m]$ are modal mass and modal stiffness matrices, respectively. Mass normalising the modal matrix by

$$\Psi_{ij} = \frac{\phi_{ij}}{\sqrt{m_{ij}}} \tag{14}$$

where Ψ_{ij} is mass normalised mode vector. By using the transformation

$$q_A = \Psi_A s_A \tag{15}$$

By premultiplying Ψ_A^T and substituting Eq. (15), Eq. (8) becomes

$$I \ddot{s}_A + \omega_A^2 s_A = \Psi_A^T f_A(t), \tag{16}$$

where ω_A^2 is a diagonal matrix comprising the eigenvalues of A .

3.1. Coupling of the components

Consider two components A and B connected together via springs, as illustrated in Fig. 3. The kinetic and strain energy of the two components, in terms of principal modal coordinates, can be given as

$$\begin{aligned} T &= \frac{1}{2} \dot{s}^T \mathbf{M} \dot{s} \\ U &= \frac{1}{2} s^T \mathbf{K} s, \end{aligned} \tag{17}$$

where T and U are kinetic and strain energy, respectively. \mathbf{M} and \mathbf{K} in Eq. (17) are

$$\mathbf{M} = \begin{bmatrix} I & 0 \\ 0 & I \end{bmatrix} \quad \mathbf{K} = \begin{bmatrix} \omega_A^2 & 0 \\ 0 & \omega_B^2 \end{bmatrix}. \tag{18}$$

The strain energy of the connectors, in terms of principal modal coordinates, is

$$U_C = \frac{1}{2} s^T \Psi^T \mathbf{K}_C \Psi s, \tag{19}$$

where \mathbf{K}_C is the connector matrix comprising the cracked nodal element's stiffness matrix which can be calculated by using Eq. (6). Ψ in Eq. (19) can be written as

$$\Psi = \begin{bmatrix} \Psi_A & 0 \\ 0 & \Psi_B \end{bmatrix}. \tag{20}$$

Table 1
Natural frequencies of the cracked Timoshenko beam for $\xi/L = 0.20$

Nat. freqs	ξ/L ratio	a/b ratio 0.20	a/b ratio 0.40	a/b ratio 0.60	a/b ratio 0.80	Intact beam
1st mode	0.20	1020.137	966.9525	842.2205	551.0463	1037.0189
2nd mode	0.20	6457.396	6454.483	6448.175	6436.008	6458.3438
3rd mode	0.20	17 872.91	17 596.57	16 944.56	15 512.55	17 960.564
4th mode	0.20	34 553.13	33 100.42	29 796.26	25 182.06	34 995.429

Table 2
Natural frequencies of the cracked Timoshenko beam for $\xi/L = 0.40$

Nat. freqs	ξ/L ratio	a/b ratio 0.20	a/b ratio 0.40	a/b ratio 0.60	a/b ratio 0.80	Intact beam
1st mode	0.40	1030.095	1006.856	942.7322	724.2739	1037.0189
2nd mode	0.40	6389.394	6174.539	5689.841	4728.978	6458.3438
3rd mode	0.40	17 844.86	17 499.83	16 792.25	15 606.35	17 960.564
4th mode	0.40	34 866.97	34 420.09	32 971.51	29 180.94	34 995.429

Table 3

Natural frequencies of the cracked Timoshenko beam for $\xi/L = 0.60$

Nat. freqs	ξ/L ratio	a/b ratio 0.20	a/b ratio 0.40	a/b ratio 0.60	a/b ratio 0.80	Intact beam
1st mode	0.60	1035.284	1029.262	1010.864	920.7848	1037.0189
2nd mode	0.60	6365.914	6071.655	5371.803	3798.216	6458.3438
3rd mode	0.60	17 807.94	17 359.27	16 478.82	15 153.19	17 960.564
4th mode	0.60	34 895.50	34 572.37	33 710.43	31 412.07	34 995.429

Table 4

Natural frequencies of the cracked Timoshenko beam for $\xi/L = 0.80$

Nat. freqs	ξ/L ratio	a/b ratio 0.20	a/b ratio 0.40	a/b ratio 0.60	a/b ratio 0.80	Intact beam
1st mode	0.80	1036.884	1036.414	1034.943	1026.769	1037.0189
2nd mode	0.80	6440.057	6375.921	6174.710	5169.264	6458.3438
3rd mode	0.80	17 758.61	17 077.99	15 286.83	11 353.18	17 960.564
4th mode	0.80	34 393.87	32 639.52	29 529.79	26 230.83	34 995.429

The total strain energy of the system is, therefore,

$$U_T = \frac{1}{2} s^T (\mathbf{K} + \Psi^T \mathbf{K}_C \Psi) s, \quad (21)$$

where \mathbf{K} has been given by Eq. (18). The equation of motion of the complete structure is

$$\ddot{s} + (\mathbf{K} + \Psi^T \mathbf{K}_C \Psi) s = \Psi^T f(t), \quad (22)$$

where Ψ has been given by Eq. (20), $f(t)$ is the global force vector for the system. From Eq. (22) the eigenvalues and eigenvectors of the cracked system can be determined. After solving this equation, the displacements for each component are calculated by using Eq. (15).

4. Results and discussion

The method described has been applied to a cracked Timoshenko beam as shown in Fig. 1 in which $L = 0.2$ m, $b = 0.0078$ m, $d = 0.025$ m. Calculation has been performed with the numerical values, $E = 216 \times 10^9$ Nm⁻², $\nu = 0.28$ and $\rho = 7.85 \times 10^3$ kgm⁻³. The finite element solutions are compared with a proprietary software in order to check the accuracy of the model the four lowest eigenfrequencies for various crack position and crack ratios are examined. In Tables 1–4 the first four smaller eigenfrequencies of the cracked Timoshenko beam and intact beam have been given for various crack positions and crack ratios. Fig. 4 shows a plot of the ratio of the first natural

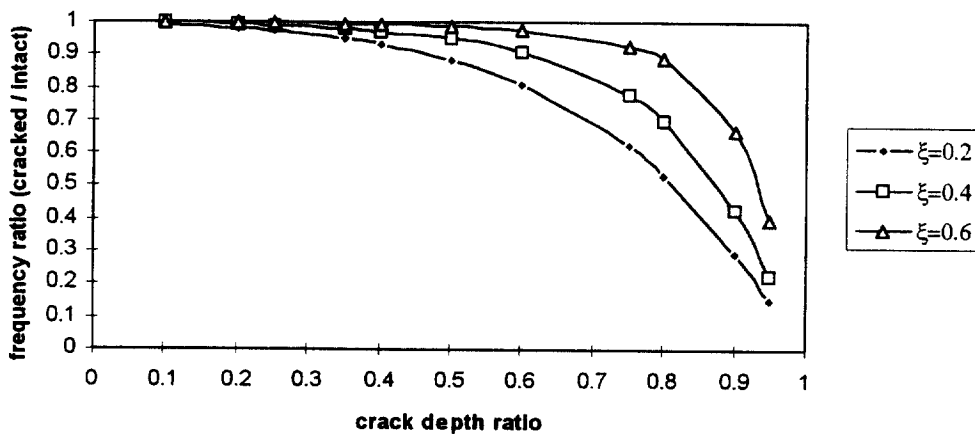


Fig. 4. Fundamental (first) frequency ratios for different crack positions.

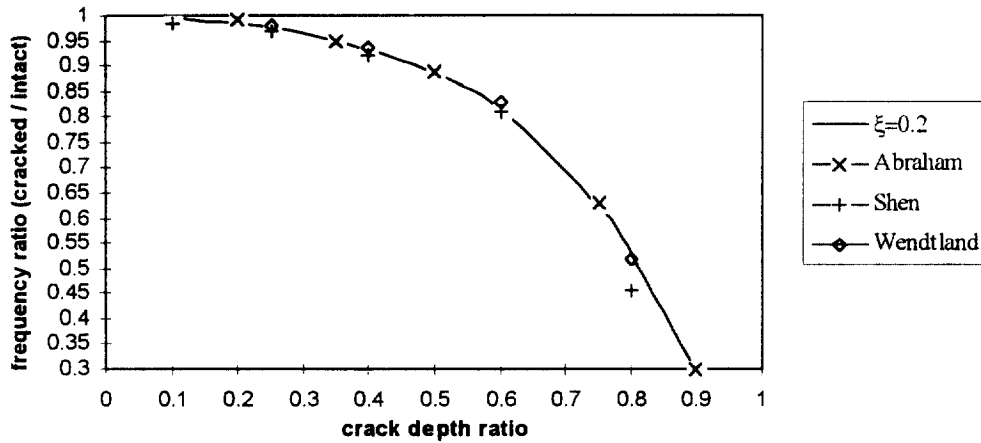


Fig. 5. Change in the fundamental natural frequency in terms of crack ratio.

frequency of the cracked beam respectively to the first natural frequency of the corresponding intact Timoshenko beam as a function of the crack depth ratio a/b for several crack positions. The natural frequencies of the cracked beam are lower than the natural frequencies of the corresponding intact beam, as expected. These differences increase with the depth of the crack. Due to the bending moment along the beam, which is concentrated at the fixed end, a crack near the free end will have a smaller effect on the fundamental frequency than a crack closer to the fixed end and it can be said that the frequencies are almost unchanged when the crack is located away from the fixed end.

The results are compared with the experimental data obtained by Wendtland [23] and theoretical data obtained by Abraham [24] and Shen [25] as shown in

Fig. 5 and 6. The first, second and third modes are shown on Fig. 7–9 for a crack respectively at $\xi = 0.2 L$, $\xi = 0.4 L$ and $\xi = 0.6 L$ when the crack depth ratio takes the values $a/b = 0.2$, $a/b = 0.4$ and $a/b = 0.6$.

5. Concluding remarks

In the methods observed in the literature compromises have been made either in the representation of the physics of the nonlinearities in defective structures or in the complexity of the structure which can be analysed. For example, finite element studies usually use a simplistic representation of the interface mechanics whereas analytical studies require simple boundary conditions. Neither is satisfactory in

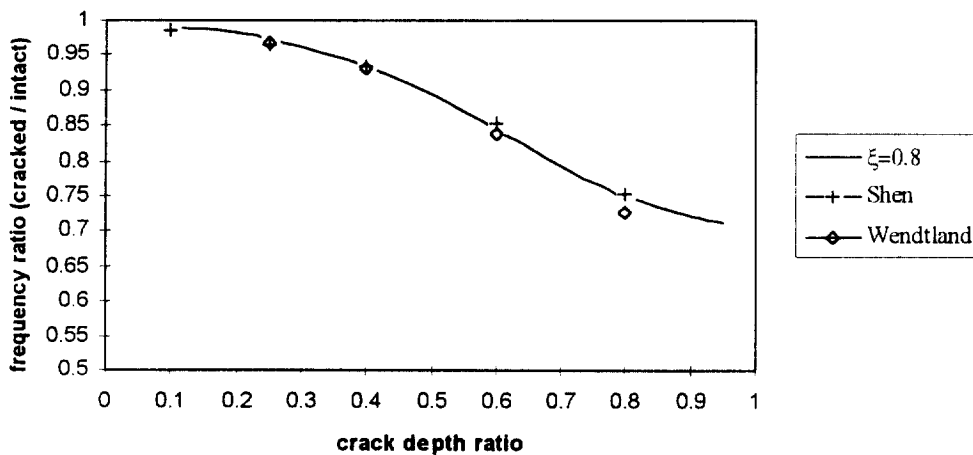


Fig. 6. Change in the fourth natural frequency in terms of crack ratio.

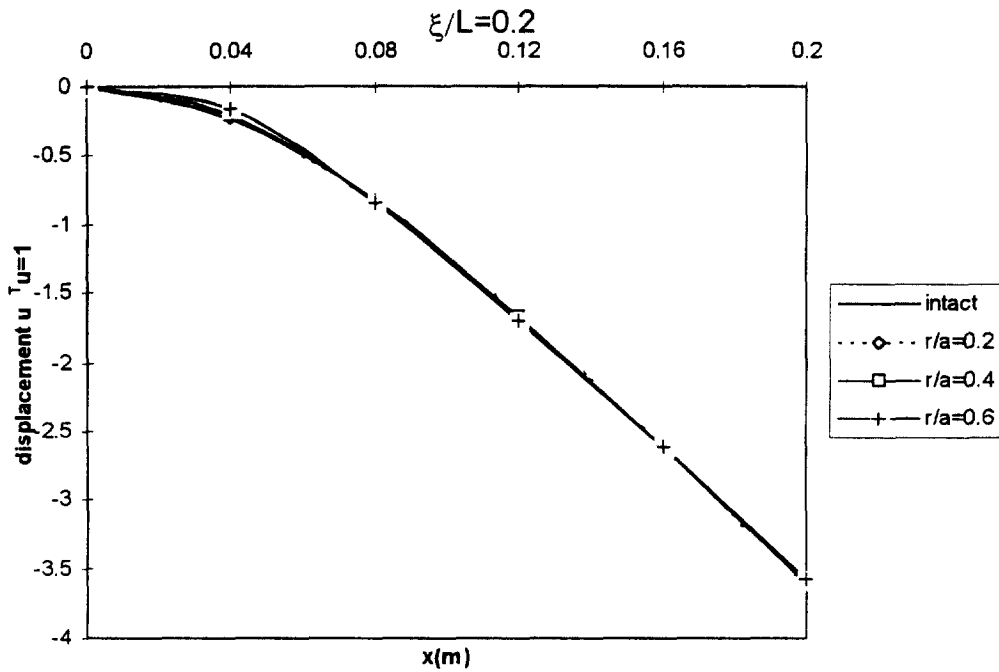


Fig. 7. First mode shapes of cracked beam for $\xi/L=0.2$ and $r/a=0.2, 0.4, 0.6$.

isolation in practical design studies. It is believed that the current approach addresses both of these issues leading to the development of design tools which are capable of accurate analysis of nonlinear interface

effects. To illustrate the effectiveness of the approach, results have been compared with previous studies published in the literature leading to confidence in the validity of this approach.

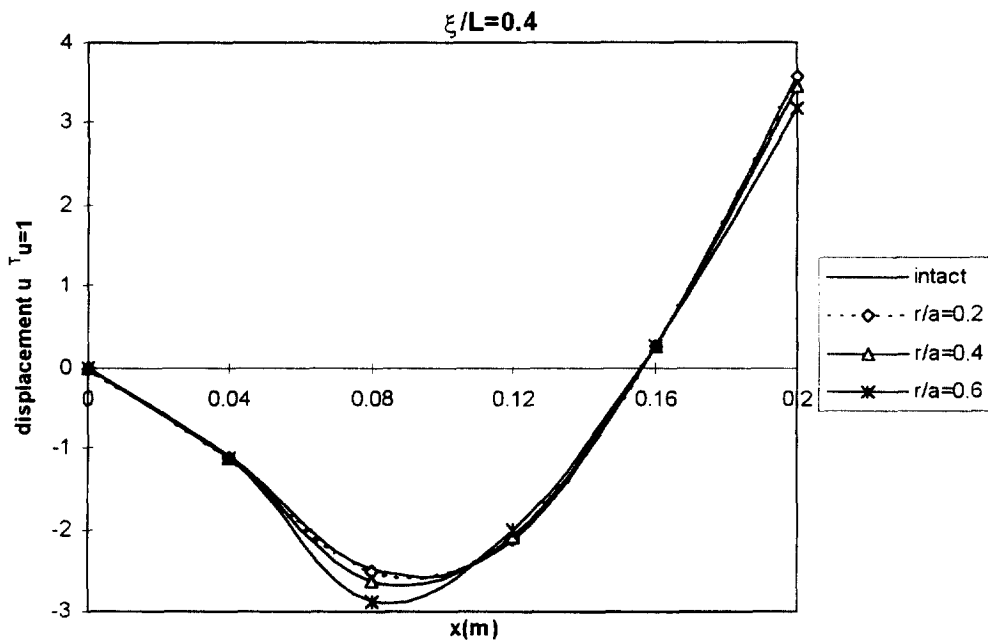


Fig. 8. Second mode shapes of cracked beam for $\xi/L=0.4$ and $r/a=0.2, 0.4, 0.6$.

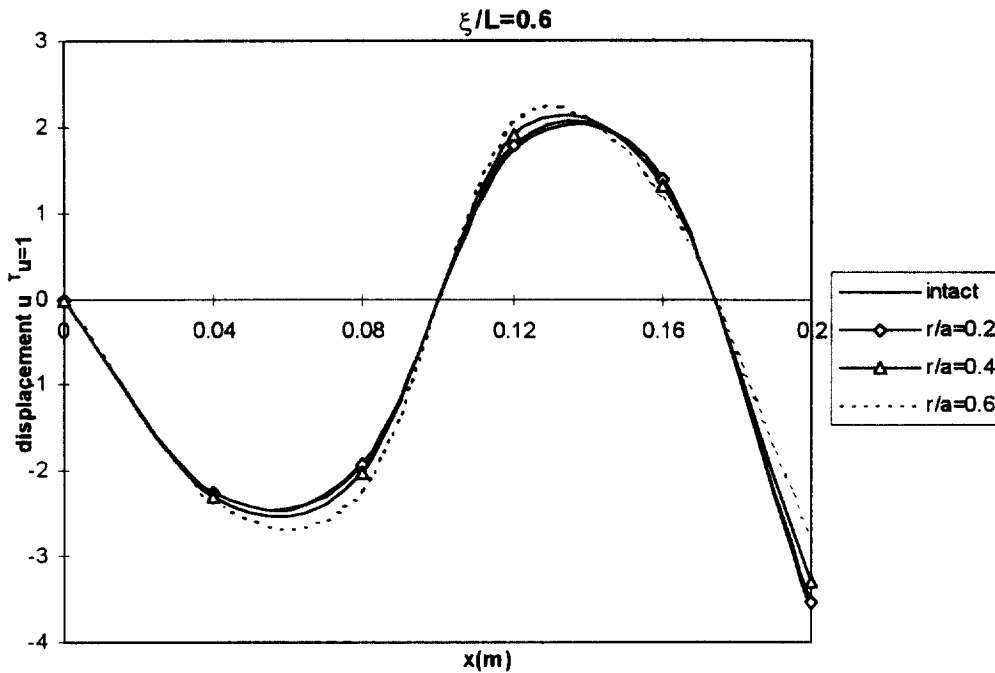


Fig. 9. Third mode shapes of cracked beams for $\xi/L=0.6$ and $r/a=0.2, 0.4, 0.6$.

References

- [1] Gudmundson P. Eigenfrequency changes of structures due to cracks, notches or other geometrical changes. *J Mech Phys Solids* 1982;30:339–53.
- [2] Gudmundson P. The dynamic behaviour of slender structures with cross-sectional cracks. *J Mech Phys Solids* 1983;31:329–45.
- [3] Cawley P, Adams RD. The location of defects in structures from measurements of natural frequencies. *J Strain Analysis* 1979;14:49–57.
- [4] Yuen MMF. A numerical study of the eigenparameters of a damaged cantilever. *J Sound Vibr* 1985;103:301–10.
- [5] Gounaris G, Dimarogonas AD. A finite element of a cracked prismatic beam for structural analysis. *Comput Struct* 1988;28:309–13.
- [6] Qian GL, Gu SN, Jiang JS. The dynamic behaviour and crack detection of a beam with a crack. *J Sound Vibr* 1990;138:233–43.
- [7] Rizos PF, Aspragathos N, Dimarogonas AD. Identification of crack location and magnitude in a cantilever beam from the vibration modes. *J Sound Vibr* 1990;138:381–88.
- [8] Shen MHH, Taylor JE. An identification problem for vibrating cracked beams. *J Sound Vibr* 1991;150:457–84.
- [9] Shen MHH, Chu YC. Vibrations of beams with a fatigue crack. *Comput Struct* 1992;45:79–93.
- [10] Ruotolo R, Surace C, Crespo P, Storer D. Harmonic analysis of the vibrations of a cantilevered beam with a closing crack. *Comput Struct* 1996;61:1057–74.
- [11] Abraham ONL, Brandon JA. The modelling of the opening and closure of a crack. *J Vibr Acoustics-Trans ASME* 1995;117:370–7.
- [12] Abraham ONL, Brandon JA. The modelling of a “breathing” cracked beam. *European Mechanics Colloquium, Euromech 280, Identification of non-linear Mechanical Systems from Dynamic Tests*, Ecole Centrale de Lyon. Rotterdam: AA Balkema, 1992:43–50.
- [13] Brandon JA, Abraham ONL. Counter-intuitive quasi-periodic motion in the autonomous vibration of cracked Timoshenko beams. *J Sound Vibr* 1995;185:415–30.
- [14] Hurty WC. Dynamic analysis of structures using sub-structure modes. *AIAA J* 1965;3:678–85.
- [15] Ewins DJ. *Modal testing: theory and practice*. England: Research Studies Press Ltd, 1984.
- [16] Martin KF, Ghilaim KH. System prediction using damped component modes. *Proc Instn Mech Engrs Part C* 1984;198:261–68.
- [17] Ghilaim KH. *Modal techniques in system approximation*. PhD thesis. University of Wales College of Cardiff, 1984.
- [18] Moon JD, Cho DW. A component mode synthesis applied to mechanism for an investigation of vibration. *J Sound Vibr* 1992;157:67–79.
- [19] Nobari AS, Robb DA, Ewins DJ. The influence of joints in structural dynamic coupling analysis. In: *Proceedings of the 17th International Seminar on Modal Analysis*. Belgium: Leuven KP, 1992;Vol. 2:825–43.
- [20] Gounaris G, Papazoglou V. Three-dimensional effects on the natural vibrations of cracked Timoshenko beams in water. *Comput Struct* 1992;42:769–79.
- [21] Weaver W, Jonston PR. *Finite element for structural analysis*. Englewood Cliffs, NJ: Prentice-Hall, 1984.

- [22] Papadopoulos CA, Dimarogonas AD. Coupled longitudinal and bending vibrations of a rotating shaft with an open crack. *J Sound Vibr* 1987;117:81–93.
- [23] Wendtland D. Änderungen der Biegeeigenfrequenzen einer idealisierten schaufel durch risse. PhD thesis. Universität Karlsruhe, 1972.
- [24] Abraham ONL. 1993. Dynamic modelling of cracked Timoshenko beams. PhD thesis. University of Wales College of Cardiff.
- [25] Shen MHH. Natural modes of Bernoulli–Euler beams with symmetric cracks. *J Sound Vibr* 1990;138: 115–34.